Reliable Identification of Damage Growth Using Guided Wave SHM Systems

Andrea Galvagni, Peter Cawley

RELIABLE IDENTIFICATION OF DAMAGE GROWTH USING GUIDED WAVE SHM SYSTEMS

Andrea Galvagni[1], Peter Cawley[1]

[1] *Department of Mechanical Engineering, Imperial College, London SW7 2AZ, UK*

p.cawley@imperial.ac.uk

ABSTRACT

A practical guided wave SHM system will be interrogated frequently and this will generate a large volume of data that must be processed. This paper discusses the use of sequential analysis to assess whether a change has occurred and whether it is of a form consistent with damage growth, rather than environmental changes. A methodology based on the generalised likelihood ratio (GLR) algorithm is introduced and applied to the guided wave monitoring of an 8 inch diameter pipe loop which is subjected to temperature cycling and the introduction of damage at different locations along the pipe. It is shown that the GLR algorithm can be used to process the signals automatically and to identify damage at specified probability of detection (POD) and probability of false alarm (PFA) rates. It is possible to detect damage corresponding to 0.25% cross section area loss in regions remote from features and to 0.5-0.75% loss at other locations. The methodology promises to be an important tool in the practical implementation of guided wave SHM.

KEYWORDS : *guided wave, PIMS, sequential analysis, GLR algorithm*

1 INTRODUCTION

There is increasing interest in employing permanently installed Structural Health Monitoring (SHM) systems as an alternative to periodic inspection of safety-critical structures [1]. SHM systems using guided ultrasonic waves have attracted particular attention, mainly due to their ability to cover relatively large areas of the structure and provide good defect localization capability with a reduced number of sensors [2-4]. However, in spite of a great deal of research effort, large area guided wave SHM deployment in industry has been limited.

The biggest commercial application of guided ultrasonic waves is for the periodic inspection of pipelines in the petrochemical industry, and they are increasingly used in the power sector as well [5]. The main advantage of the method is its ability to screen many metres of pipe from a single transduction location, resulting in substantial time and cost savings. Standard guided ultrasonic wave inspection works by transmitting a single guided wave mode (usually the torsional mode [5]) and identifying the reflections from any discontinuities in the pipe. This approach assumes that each echo in the recorded signal is distinct from all others and is free from interference and coherent noise; in the case of pipelines it is typically very effective due to the one-dimensional nature of these structures and their relatively low feature density. However, the ability to detect damage occurring at a feature such as a weld is limited since an echo is obtained even from a good weld, so damage is only seen if the signal can be identified as abnormal. In complex lines with multiple features such as tees, diameter changes, bends etc, the echoes from different features may overlap and interfere with each other, making reliable detection more difficult. Furthermore, the sensitivity of ultrasonic guided wave inspection to small discontinuities is limited, since it is necessary for a discontinuity to reflect a wave packet of greater magnitude than the underlying noise floor for it to be detectable.

Pipes are often buried, submerged or too high for access without scaffolding, making it difficult and expensive to gain access to even a single location along them; in these circumstances, if regular inspection is required, it becomes very attractive to attach a permanently installed guided wave monitoring system (PIMS), to the pipeline. The sensor can then be remotely operated from a convenient location and there is no need to access the pipe after sensor installation unless damage develops. In addition to reducing access costs for repeat inspections, PIMS allows highly accurate repeat measurements and so converts the one-off inspection performed with the conventional guided wave inspection technology [5] to a guided wave health monitoring system. This enables the use of baseline subtraction techniques to track changes in the signal received by the sensor, and thus ultimately changes in the structural condition of the pipe. In principle, this enables smaller defects to be found than is possible in a one-off inspection, and for defects to be found more reliably in the vicinity of pipe features, though baseline subtraction is far from trivial [6, 7]. However, there is currently no accepted technique for identifying the onset of damage at a required probability of detection (POD) and false alarm rate (PFA); this is essential if the method is to find widespread use, and this paper presents a methodology for achieving this.

The methodology can be applied to any guided wave inspection system but in order to make the processing involved clearer, it is presented in the context of a controlled trial of a PIMS system. Section 2 describes the test setup and the initial baseline subtraction processing to give residual signals in which any damage growth is to be identified; Section 3 then discusses the identification of changes in the signals at specified POD and PFA levels via sequential analysis. The results obtained with signals acquired on the test installation are presented in Section 4, and conclusions and implications for practical testing are given in Section 5. More details of the work can be found in [8].

2 EXPERIMENTS

2.1   Test Setup

Tests were carried out on a test loop comprising an 8 inch nominal bore, schedule 40 (8mm wall thickness) steel pipe, the section of interest being shown schematically in Fig 1. Two PIMS sensors (Guided Ultrasonics Ltd) were bonded to the pipe at the locations shown in Fig 1, only sensor P1 being used in the tests reported here. The pipe section of interest was held by four clamped supports that were lined with silicone rubber and produced minimal reflections of the guided waves; the other side of the loop had rigidly clamped glass fibre reinforced plastic (GRP) supports that gave a significant reflection. The temperature of the pipe loop could be varied via heating blankets surrounding the pipe and was computer controlled.

Initially, a set of four readings was collected from sensor P1 while the pipe loop was at 100^0F and in a baseline, damage-free condition. Subsequently, damage in the form of 1 inch diameter, machined flat-bottomed holes was introduced in the pipe loop at locations A, B and C indicated in Fig 1. The three locations were chosen to simulate three different damage detection scenarios of increasing difficulty. At location A, damage is introduced in a free section of pipe and therefore its echo should be easy to detect because it can only be masked by coherent noise but not by the large echoes from pipeline features. At location B, damage is introduced a few millimetres after a weld, and it is therefore expected to be more difficult to detect because its echo is masked by the large echo from the weld. Finally, at location C, not only is damage introduced in the vicinity of two welds, but it is also located past two welds and a bend.

The depth of the flat-bottomed holes was increased in three successive 0.25% cross-sectional area increments, removing a nominal total 0.25%, 0.5% and 0.75% cross-sectional area at each of
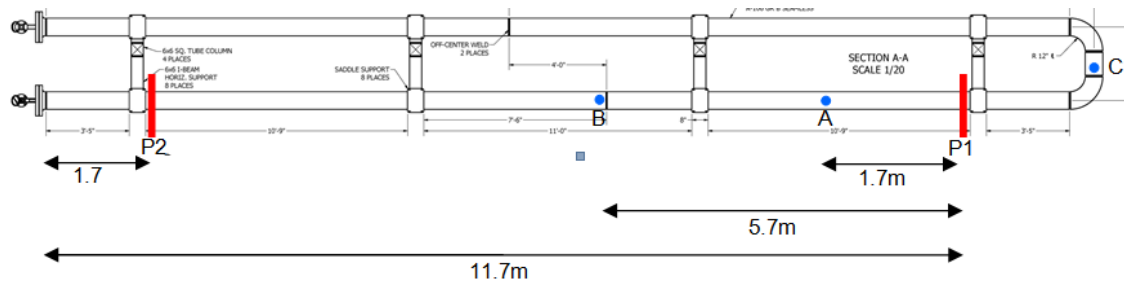
Figure 1. Schematic diagram of loop showing positions of sensors P1 and P2 (only P1 used in tests reported here) and defect locations A, B and C. Defect B was centred approximately 25 mm from the crown of the adjacent butt weld, and defect C was centred approximately 50 mm from the weld between the first elbow section beyond sensor P1 and the straight section forming the bottom of the U loop. Defect C was approximately 2.1m from sensor P1 measured along the centre line of the pipe.
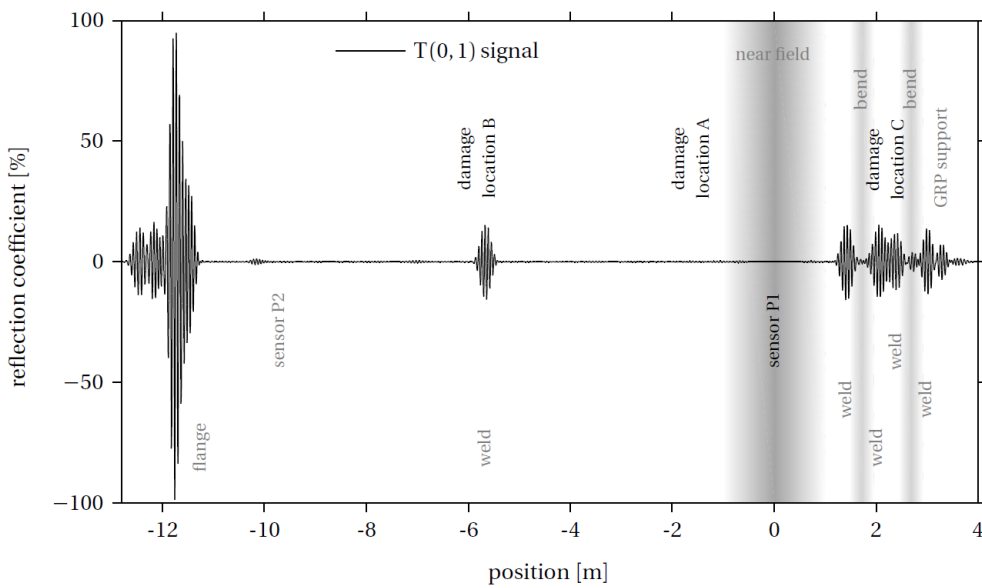

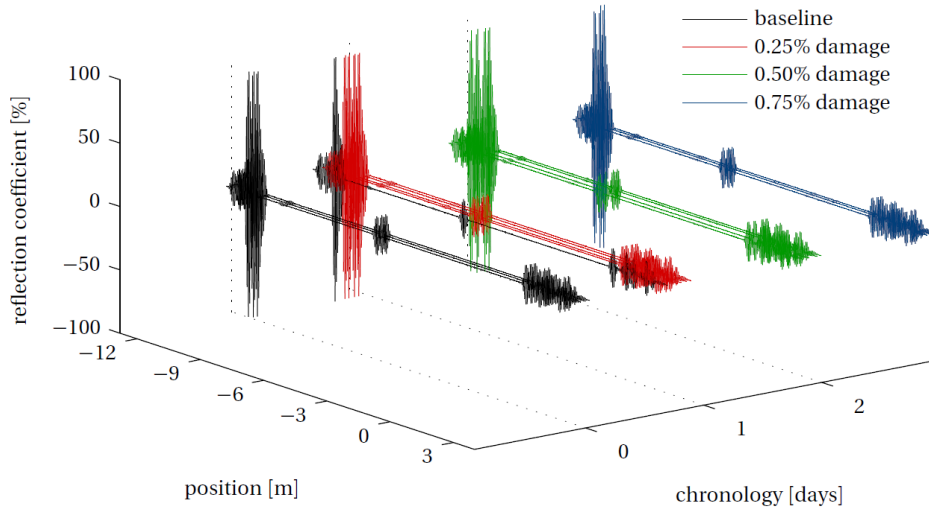Figure 2. Typical baseline signal.

Figure 3. Signals captured in baseline and three damage conditions for results reported here.

the three locations. (Measurements showed that the holes were not precisely flat bottomed so the area removed was not exactly as intended; the true areas removed are given in [8].) After each damage increment the temperature of the pipe loop was increased to 194^0F (90^0C) and subsequently returned to 100^0F (37.8^0C) before collecting a set of readings. This meant that the sensor was thermally stressed, as it would be over different seasons and operating conditions in the field.

In all the results presented here, the PIMS sensor was excited by an 8 cycle, 27 kHz (the centre frequency of the transduction system) Hann windowed toneburst to transmit a torsional, T(0,1) mode, guided wave packet along the pipe. The signals received by the sensor were processed to give the T(0,1) echoes from both directions along the pipe; since the velocity of propagation of the T(0,1) mode is known, the timebase can readily be converted to a distance scale. The excitation and reception was done with a Guided Ultrasonics Ltd G3 system and the processing to obtain the signals was the same as for the deployable testing system described in [5]. Distance-Amplitude Correction (DAC) curves are typically used in ultrasonic inspection to account for attenuation along the wave propagation path and are routinely employed in guided wave inspection [5]. The amplitude of the DAC curve is representative of the amplitude of the incident signal at any given location and this decreases with distance because of damping as well as feature reflections. Dividing the amplitude of the signal at a given location by the value of the DAC curve at the corresponding point gives the reflection coefficient as a function of position as shown in Fig 2, where the main reflectors are identified and the damage locations are shown. Fig 3 presents the T(0,1) RC signals for all the readings considered here.

2.2 Initial Signal Processing – Baseline Subtraction

Baseline subtraction involves subtracting a baseline signal, recorded when the structure under consideration is in a known condition, from the current signal; the residual signal left after subtraction should only include information about damage growth since the baseline was recorded [6, 7]. Importantly, this removes the need to interpret and separate in time the reflections from different features, as only damage information is shown. Baseline subtraction assumes that the reflections from features remain constant over time unless further damage develops. In practice, however, factors other than the initiation and growth of damage influence feature reflections, temperature being a particularly important influence [6, 7]. Even though the results presented here were collected at nominally constant temperature it was found to be important to apply compensation, the baseline stretch method being employed, essentially as described in [7].

3 IDENTIFICATION OF DAMAGE GROWTH

We want to identify the onset of change in the residual signals after baseline subtraction. This is conveniently done by applying sequential analysis in the form of the generalised likelihood ratio (GLR) algorithm [9-11]. The probability density of the residual signal at a given location along the pipe in the absence of damage is given by $p(y|\theta_0)$, while in the presence of damage it is given by $p(y|\theta_1)$. We capture a finite set $Y_n = \{y_1, y_2, ..., y_n\}$ of readings at known times $t_1, t_2,..., t_n$. We want to detect the onset of change in the probability density function and to estimate the time of change t_c and the value of θ_1, the damage signal amplitude. Consider hypothesis $\mathbf{H_0}$ that states that the probability density function of y is given by $p(y|\theta_0)$, and $\mathbf{H_1}$ that it is given by $p(y|\theta_1)$. The log likelihood ratio

$$z_i(v) = \ln \frac{p(y_i | \theta_0 + v)}{p(y_i | \theta_0)}, \quad v = \theta_1 - \theta_0 \tag{1}$$

will be a function of the value of the sample y_i and the change vector v. The cumulative log likelihood ratio is given by

$$Z_k^j(v) = \sum_{i=j}^{k} z_i(v) \qquad (2)$$

The double maximisation

$$g_k = \max_{1 \leq j \leq k} \sup_v Z_k^j(v) \qquad (3)$$

finds likeliest change vector v for which samples $y_j, y_{j+1}, \ldots, y_n$ are most likely to have probability density function $p(y|\theta_0+v)$ when samples $y_1, y_2, \ldots, y_{j-1}$ have probability density function $p(y|\theta_0)$. We prescribe probabilities $1-\beta$ of detection and α of false calling. Then hypothesis $\mathbf{H_1}$ that the probability density function has shifted to $p(y|\theta_1)$ is accepted and change is detected at sample y_d and time t_d where d is the smallest positive integer for which

$$g_d \geq lnA \qquad \text{where} \qquad A = \frac{1-\beta}{\alpha} \qquad (3)$$

The discussion above treats each position along the pipe separately. However, we know that the input signal is a windowed toneburst so we expect reflections to be of this form, centred on the feature location. Therefore in practice, we do not consider each point in isolation but look for the presence of windowed tonebursts in the residual signal centred on each point in turn. Further details are given in [8].

4   RESULTS

Fig 4 presents the baseline residual RC signals obtained from all the baseline and damage signals of Fig 3. As can be seen from Fig 4, in both the baseline and the damage residuals there are large echoes corresponding to the flange near -12m and to the GRP support near 3m. It is common for the residual signal to have a large magnitude at the locations of complex features as result of the imperfect subtraction of their echoes [7]. Importantly, Fig 4 reveals that near locations A, B and C there are differences between the baseline and the damage residuals as a result of the introduction of damage but these differences are smaller than some of those at other locations where there is no damage, so if a simple threshold were to be used there would be either missed defects or false calls.
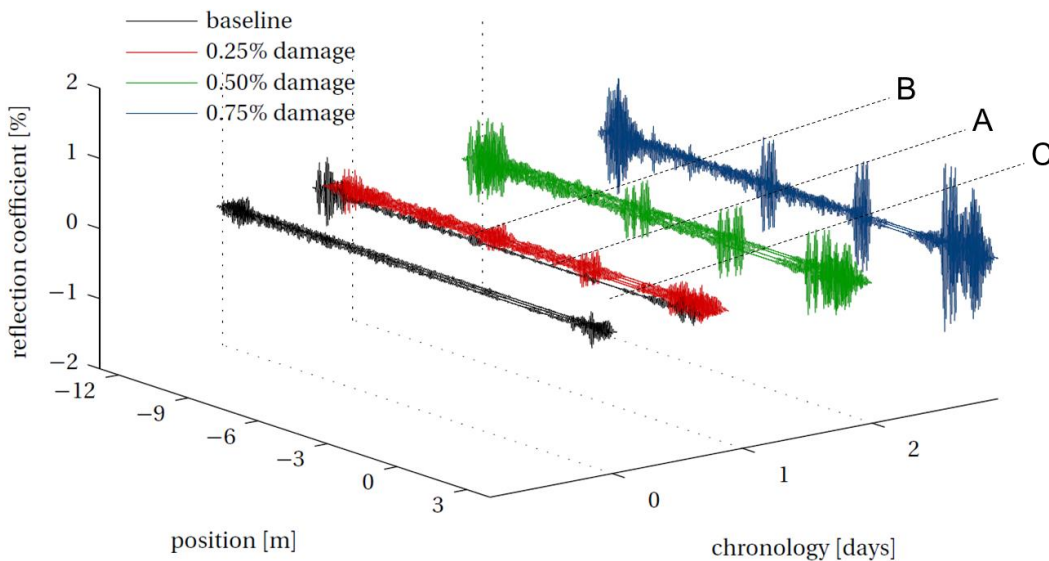

Figure 4. Baseline residual signals corresponding to raw signals of Figure 3.
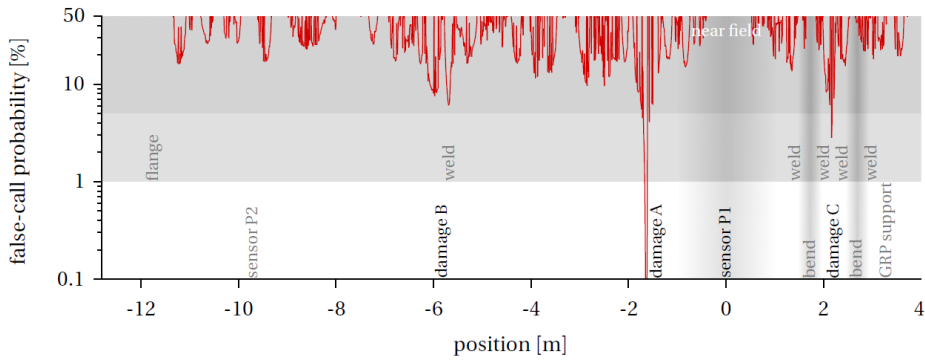
Figure 5. Acceptable false call probability level required to make change at each position 'callable' at 99.9% POD in case of 0.25% cross section loss at A, B and C.
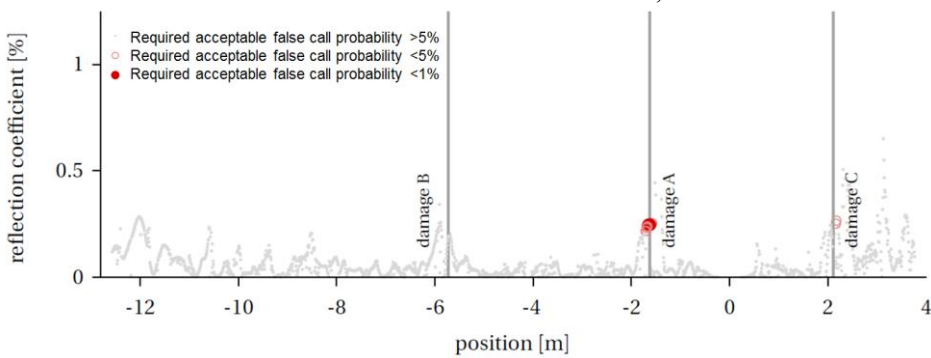

Figure 6. Estimated reflection coefficient at each position from results of Figure 5.
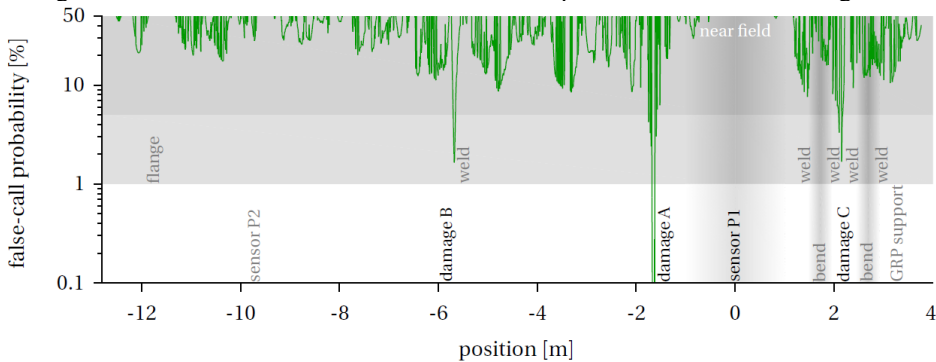

Figure 7. As Figure 5 with 0.5% cross section loss at A, B and C.
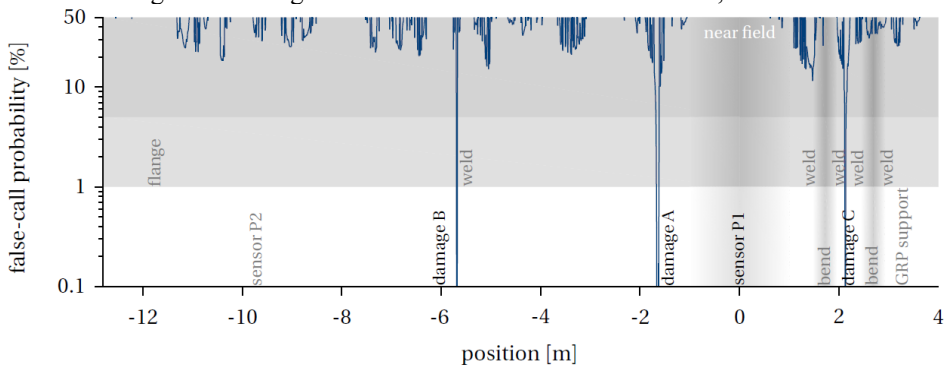

Figure 8. As Figure 5 with 0.75% cross section loss at A, B and C.

As a result, without prior knowledge about the introduction of damage, it becomes very difficult to establish whether there is any echo from damage growth and where it is located. The change detection procedure of Section 3 is therefore required to assess whether damage is present. In normal operation, this would be done by specifying the required POD and acceptable false call rate and investigating whether damage was detected and whether there were any false calls. In order to give a better picture of the operation of the algorithm, here we set the required POD very high at 99.9% and plot the false call level that must be allowable to make change at each location along the pipe 'callable'. This is done by rearranging equation (3) and recognising that at the margin of calling, $g_d=lnA$, so for a given POD requirement $1-\beta$,

$$\alpha = (1-\beta)\exp(-g_k) \qquad (4)$$

Fig 5 shows the acceptable false call probability level, α, from equation (4) required to make change at each position 'callable' at 99.9% POD for the case of 0.25% cross section loss at positions A, B and C using four baseline readings and four 'damage' readings (the black and red signals from Fig 4). Fig 6 shows the corresponding results for the estimated amplitude of the damage echo. It can be seen in Fig 5 that the only position where the probability of false-call falls to negligible levels is in the vicinity of location A. Similarly, Fig 6 shows that where there is a low probability of false-call, *i.e.* in the vicinity of location A, the estimated amplitude of the damage echo is approximately 0.25%, corresponding to the nominal 0.25% cross-sectional area loss. (Since the damage axial length is around a quarter of the wavelength of the incident T(0,1) guided wave packet, the reflection coefficient is approximately the same as the % cross section loss [12].) Importantly, none of the large residuals corresponding to the flange and the GRP support in Fig 2 are identified as an indication of potential damage growth.

Fig 7 shows the results corresponding to Fig 5 for the case of nominal 0.5% damage. As in Fig 5, the only position where the acceptable false call probability required to make the damage callable is negligible is in the vicinity of location A; however, the damage at B and C would be 'callable' at an acceptable false call probability of around 2%. The corresponding results with nominal 0.75% damage are shown in Fig 8 (only three readings were taken in this condition). In this case the acceptable false call probability required to make the damage callable is negligible in the vicinity of locations A, B and C so 0.75% damage in the vicinity of features is detectable with minimal cost in terms of false calls at other locations.

CONCLUSION

A practical permanenly installed guided wave pipe inspection system has been trialled on a realistic test loop and the results processed using sequential analysis to assess whether a change has occurred and whether it is of a form consistent with damage growth, rather than environmental changes. It has been shown that the generalised likelihood ratio (GLR) algorithm can be used to process the signals automatically and to identify damage at specified probability of detection (POD) and probability of false alarm (PFA) rates. It is possible to detect damage corresponding to 0.25% cross section area loss in regions remote from features and to 0.5-0.75% loss at other locations. The methodology promises to be an important tool in the practical implementation of guided wave SHM.

ACKNOWLEDGEMENTS

REFERENCES

[1]   C. Boller, Next generation structural health monitoring and its integration into aircraft design, *International Journal of Systems Science*, 31, 1333–1349, 2000.

[2]   X. Zhao, H. Gao, G. Zhang, B. Ayhan, F. Yan, C. Kwan and J.L. Rose, Active health monitoring of an aircraft wing with embedded piezoelectric sensor/actuator network: I. Defect detection, localization and growth monitoring, *Smart Materials and Structures,* 16, 1208-1217, 2007.

[3]   J.-B Ihn, and F.-K. Chang, Pitch-catch active sensing methods in Structural Health Monitoring, *Structural Health Monitoring*, 7, 5-19, 2008.

[4]   J.S. Hall and J.E. Michaels, Minimum Variance Ultrasonic Imaging Applied to an *In Situ* Sparse Guided Wave Array, *IEEE Trans UFFC*, 57, 2311-2323, 2010.

[5]   D.N. Alleyne, B. Pavlakovic, M.J.S Lowe, and P Cawley. 'Rapid long-range inspection of chemical plant pipework using guided waves', *Insight*, 43, 93-96,101, 2001.

[6]   Y. Lu and J.E. Michaels, A methodology for structural health monitoring with diffuse ultrasonic waves in the presence of temperature variations, *Ultrasonics*, 43, 717-731, 2005.

[7]   T. Clarke, P. Cawley, P. D. Wilcox and A. J. Croxford, Evaluation of the damage detection capability of a sparse array guided wave SHM system applied to a complex structure under varying thermal conditions, *IEEE Trans. Ultrason., Ferroelect., Freq. Contr.* 56, 2666-2678, 2009.

[8]   A. Galvagni, Pipeline Health Monitoring, *EngD thesis*, Imperial College London, 2013.

[9]   D.L. Burkholder and R.A. Wijsman, Optimum properties and admissibility of sequential tests, *Ann Math Stat*, 34, 1-17, 1963.

[10]   B. Eisenberg, B.K. Ghosh and G. Simons, Properties of generalized sequential probability ratio tests, *Ann Stat*, 4, 237-251, 1976.

[11]   A. wald and J. Wolfowitz, Optimum character of the sequential probability ratio test, *Ann Math Stat*, 19, 326-339, 1948.

[12]   A. Lovstad and P. Cawley, The reflection of the fundamental torsional guided wave from multiple circular holes in pipes, *NDT&E International*, 44, 553-562, 2011.